*Citation for published version:*
Ma, X, Suturina, EA, Rouzières, M, Platunov, M, Wilhelm, F, Rogalev, A, Clérac, R & Dechambenoit, P 2019, 'Using Redox-Active bridging Ligand as a Control Switch of Intramolecular Magnetic Interactions', *Journal of the American Chemical Society*, vol. 141, no. 19, pp. 7721-7725. https://doi.org/10.1021/jacs.9b03044

*DOI:*
10.1021/jacs.9b03044

*Publication date:*
2019

*Document Version*
Peer reviewed version

# Using Redox-Active π Bridging Ligand as a Control Switch of Intramolecular Magnetic Interactions

Xiaozhou Ma,[†,‡] Elizaveta A. Suturina,[#] Mathieu Rouzières,[†,‡] Mikhail Platunov,[⊥] Fabrice Wilhelm,[⊥] Andrei Rogalev,[⊥] Rodolphe Clérac,*[,†,‡] and Pierre Dechambenoit*[,†,‡]

[†] CNRS, CRPP, UMR 5031, Pessac F-33600, France

[‡] Univ. Bordeaux, CRPP, UMR 5031, Pessac F-33600, France

[#] Centre for Sustainable Chemical Technologies (CSCT), University of Bath, Claverton Down, Bath BA2 7AY, UK

[⊥] ESRF-The European Synchrotron, CS 40220, 38043 Grenoble Cedex 9, France

S *Supporting Information*

**ABSTRACT:** Intramolecular magnetic interactions in the dinuclear complexes $[(\text{tpy})\text{Ni}(\text{tphz})\text{Ni}(\text{tpy})]^{n+}$ ($n$ = 4, 3 and 2; tpy: terpyridine; tphz: tetrapyridophenazine) were tailored by changing the oxidation state of the pyrazine-based bridging ligand. While its neutral form mediates a weak antiferromagnetic (AF) coupling between the two $S = 1$ Ni(II), its reduced form, tphz$^{\bullet-}$, promotes a remarkably large ferromagnetic exchange of +214(5) K with Ni(II) spins. Reducing twice the bridging ligand affords weak Ni-Ni interactions, in marked contrast to the Co(II) analogue. Those experimental results, supported by a careful examination of the involved orbitals, provide a clear understanding of the factors which govern the strength and sign of the magnetic exchange through an aromatic bridging ligand, a prerequisite for the rational design of strongly coupled molecular systems and high $T_C$ molecule-based magnets.

The efficient control of the interactions between magnetic centers is a fascinating challenge, at the basis of any possible rational design of molecule-based magnets.[1] This fundamental problem is intrinsically linked to the question of the relative localization (or delocalization) of the unpaired electrons. Those are often located on *d* (or *f*) orbitals of metal ions, and interact weakly by superexchange through diamagnetic bridging ligands or atoms. Nevertheless, two alternative strategies have received recently an increasing interest to promote strong magnetic coupling: (i) the mixed valence approach, for which an electron delocalization promotes double exchange, which exceeds the superexchange;[2] and (ii) the radical bridge approach, where an organic radical ligand is placed between paramagnetic metal centers, acting as a magnetic relay.[3] For the latter, the organic bridge characteristics are crucial to optimize the strength of the magnetic interactions: it should be strongly coordinating to ensure an efficient mixing of the involved metal/organic orbitals,[3d,4] and its unpaired electron should be as delocalized as possible between the paramagnetic metal ions.

Based on these prerequisites, our group recently reported[4] a prototype dinuclear complex based on Co(II) and the redox-active tphz bridging ligand.[5] In this system, the intramolecular magnetic interactions are controlled by successive reduction processes. While the neutral form of tphz mediates a weak AF exchange between *ls*-Co(II) (*ls*: low-spin), the once reduced radical form stabilizes very strong AF couplings between the $S = {}^{1}/_{2}$ organic spin and the two *hs*-Co(II) (*hs*: high-spin). The resulting high-spin complex possesses a well isolated $S_T = {}^{5}/_{2}$ ground state that is remarkably the only thermally populated state at ambient temperature. When further reducing this dinuclear complex, despite the formal diamagnetic state of the tphz$^{2-}$ ligand, a strong AF coupling between two *hs*-Co(II) is observed, leading to an overall non-magnetic ground state. In this case, the strong magnetic interaction is induced by a large spin delocalization arising from an efficient orbital mixing of the tphz$^{2-}$ π system and one of the Co(II) singly occupied *d* orbitals. Therefore, in this type of radical/metal ion complexes, the nature and magnitude of the intramolecular coupling is indeed predictable based on both electronic configurations of metal ions and the bridging ligand.

To further experimentally investigate the role of the metal/organic orbital complementarity in the control of the magnetic interactions, a novel family of dinuclear Ni(II) complexes was synthesized with the redox-active tphz ligand. The reaction of $\text{Ni(tpy)Cl}_2$,[6] $\text{TlPF}_6$ and tphz in $\text{CH}_3\text{CN}$ leads to a new dinuclear nickel complex that was isolated as orange needle-shaped crystals of $[\text{Ni}_2(\text{tphz})(\text{tpy})_2](\text{PF}_6)_4{\bullet}3\text{CH}_3\text{CN}$ (**1**) after slow diffusion of $\text{Et}_2\text{O}$ vapors (Supporting Information). The single crystal X-ray diffraction data at 120 K (Figure 1, Table S1) reveal that **1** is isostructural to the Co(II) analogue,[5] possessing two equivalent $\text{Ni}^{\text{II}}(\text{tpy})^{2+}$ fragments bridged by a neutral tphz ligand. The cyclic voltammetry of **1** in $\text{CH}_3\text{CN}$ reveals four one-electron redox events at -0.40, -1.25, -1.66, -1.82 V versus *vs.* $\text{Fc}^+/\text{Fc}$ (Figure 2)[7] with a rest potential at -0.15 V, indicating only reduction processes. By comparing with the reported Ru(II)[8] and Co(II)[4] analogues, the two processes at -0.40 and -1.25 V can be assigned to the reduction of the bridging ligand and the other two most cathodic ones to the tpy reduction. The large separation between the two first redox potentials evidences the high stability of the tphz radical in the complex, with a comproportionation constant of *ca.* $2.6{\times}10^{14}$. Based on these redox properties, **1** was chemically reduced with $\text{KC}_8$ to give once and twice reduced systems as $[\text{Ni}_2(\text{tphz})(\text{tpy})_2](\text{PF}_6)_3{\bullet}2\text{Et}_2\text{O}$ (**2**) and $[\text{Ni}_2(\text{tphz})(\text{tpy})_2](\text{PF}_6)_2{\bullet}\text{Et}_2\text{O}$ (**3**) (Supporting Information) with similar coordination environments in the dinuclear cationic Ni(II) complexes (Figure S1, Table S1). Nevertheless, significant differences are seen when comparing the bond distances within the bridging ligand

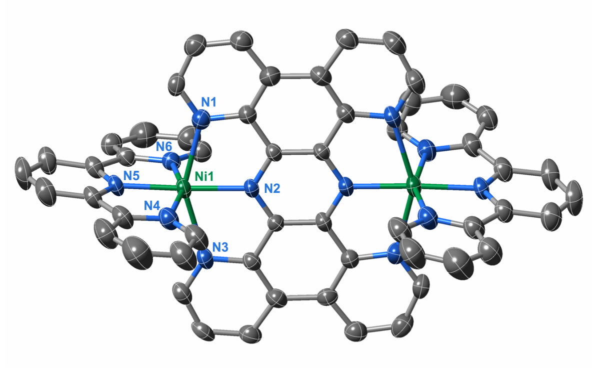

**Figure 1.** Crystal structure of $[Ni_2(tphz)(tpy)_2]^{4+}$ in **1** at 120K. Thermal ellipsoids are depicted at 50% probability level. Hydrogen atoms, solvent molecules and anions are omitted for clarity.

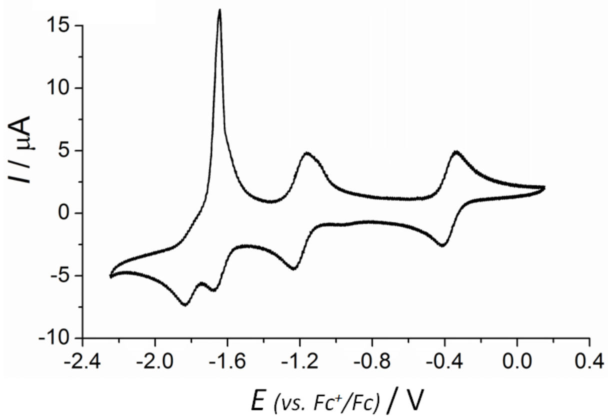

**Figure 2.** Cyclic voltammogram for a solution of **1** in $CH_3CN$ at a 0.1 V/s scan rate, and 0.1 M $(n\text{-}Bu_4N)PF_6$ as supporting electrolyte.

(Tables 1 & S2) in agreement with two successive reductions as observed for the Co series.[4] In particular, the C-N and N2⋯N2' distances in the tphz pyrazine ring are significantly elongated (Tables 1 & S2), which constitute an important signature of the successive reductions mainly centered on the bridging ligand. The Ni1-N2 distance, between the octahedral Ni site and the nitrogen atom from the tphz pyrazine ring, decreases from 1.980(4) to 1.921(4) Å upon the two reductions as a result of the increasing electrostatic interactions between the cationic metal and the bridging ligand. Those bond distances are particularly short, but in perfect agreement with the reported cobalt series.[4] The average Ni-N bond distance involving terpyridine remains quasi-unchanged upon these two first reductions, indicating the tpy redox innocence and that the Ni ion preserved its spin state and charge in agreement with CASSCF calculations (Figure S4).[9]

The local electronic and magnetic properties of the nickel metal ions were studied by X-ray absorption spectroscopy (XAS) and X-ray magnetic circular dichroism (XMCD). These techniques are particularly relevant for complexes with redox-active ligands, for which the oxidation state of the metal ion can be questioned.[10,11] The XAS spectrum at the Ni K-edge (Figure 3) is dominated by the $1s \rightarrow 4p$ transitions which show similar maxima for the three complexes between 8353.5 and 8353.8 eV. As expected for comparable coordination sphere of the probed atom, the first EXAFS (Extended X-ray Absorption Fine Structure) oscillations overlap remarkably well. The much weaker pre-edge, dipole-forbidden, $1s \rightarrow 3d$ transitions are detected at 8335.9±0.2 and 8338.9±0.3 eV for the three complexes in agreement with the expected and calculated Ni(II) ligand field splitting scheme (Figure S4).[11a] The XMCD experiments were also performed at the nickel K-edge to probe the Ni orbital magnetic moment (Figure 3). Considering that the spin–orbit interactions of the ligand atoms are negligibly small and thus cannot induce a significant orbital magnetic moment on the Ni centers, the observed XMCD signal at 8335.2±0.1 eV is only due to the orbital polarization of the $4p$ and $3d$ states induced by the intra-atomic spin–orbit coupling of the Ni atoms. The Ni magnetic moment is thus directly proportional to the XMCD signals observed in the pre-edge and edge regions. Their quasi-identical intensities demonstrate the presence of the same magnetic moment and thus spin-state on the Ni metal ions in **1**, **2** and **3**. The similarity of the XAS and XMCD spectra establishes unambiguously the identical electronic and magnetic characteristics of the Ni site in these complexes.

To quantify the strength of the intramolecular magnetic coupling, dc magnetic measurements were performed at 0.1 T (Figure 4). The $\chi T$ product of **1** remains constant between 300 and 80 K at 2.4 $cm^3Kmol^{-1}$, in good agreement with the presence of two $S = 1$ Ni(II) ($C_{Ni} = 1.2$ $cm^3Kmol^{-1}$; $g_{Ni} = 2.19(5)$). Below 80 K, the progressive decrease of $\chi T$, to a minimum value of 0.38 $cm^3Kmol^{-1}$ at 1.85K, is the result of the concerted effect of weak AF interactions between nickel spins and the Ni magnetic anisotropy. The fit of the experimental data with both contributions (solid lines in Figures 4 & S8)[12,13] gives $g_{Ni} = 2.21(5)$, $D_{Ni}/k_B = +13.6(3)$ K and $J_{Ni\text{-}Ni}/k_B = -1.86(3)$ K comparable to -4.4 K obtained by broken-symmetry DFT (B3LYP/def2-TZVP) calculations (Supporting Information).[9]

**Table 1**. Selected bond distances (Å) in **1** – **3**.

| | **1** | **2** | **3** |
|---|---|---|---|
| Ni-N1 | 2.268(5) | 2.267(7) | 2.305(4) |
| Ni-N2 | 1.980(4) | 1.962(6) | 1.921(4) |
| Ni-N3 | 2.336(5) | 2.338(7) | 2.326(4) |
| Ni-N4 | 2.089(5) | 2.097(7) | 2.100(4) |
| Ni-N5 | 1.975(4) | 2.002(6) | 1.997(3) |
| Ni-N6 | 2.078(5) | 2.084(7) | 2.114(4) |
| Ni-N(tpy)$^b$ | 2.047(5) | 2.061(7) | 2.070(4) |
| C-C(pz)$^a$ | 1.391(7) | 1.384(10) | 1.382(6) |
| C-N(pz)$^{a,b}$ | 1.331(7) | 1.359(9) | 1.375(6) |

$^a$ pz = pyrazine part of tphz; $^b$ average distance

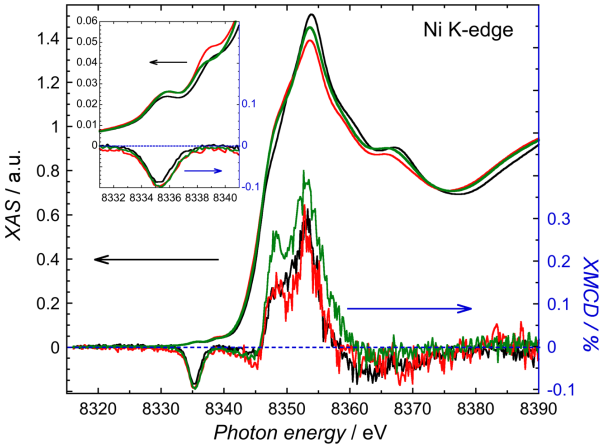

**Figure 3.** XAS and XMCD spectra at Ni K-edge for **1** (black), **2** (red) and **3** (green) at 2.5 K and 17 T. XAS spectra were normalized to zero before the edge and to unity far above the edge. XMCD spectra are given in percentage of the XAS spectra. Inset: magnification of the Ni K pre-edge region.

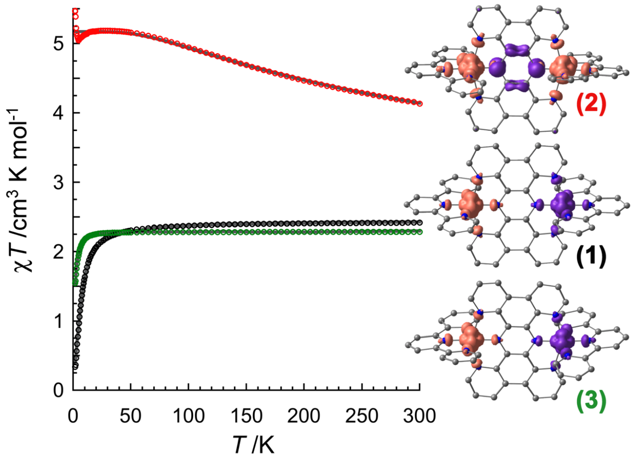

**Figure 4.** Temperature dependence of the $\chi T$ product for **1**, **2** and **3** at 0.1 T. The gray lines represent the best fits discussed in the text. Insets: view of the computed spin-density for the corresponding complexes.

For the once-reduced analogue, **2**, the $\chi T$ product at 300 K is 4.1 cm$^3$Kmol$^{-1}$, significantly higher than *ca.* 2.8 cm$^3$Kmol$^{-1}$ expected for one $S = {}^1/_2$ radical ($g_{\mathrm{rad}} = 2.0$) and two Ni(II) ($g_{\mathrm{Ni}} = 2.2$, $S = 1$ in agreement with XAS/XMCD experiments). This result suggests a remarkably strong ferromagnetic exchange between the metal ion and the bridging radical tphz$^{\bullet-}$ spins that is confirmed by the $\chi T$ increase between 300 and 40 K (Figures 4, S9). Below 40 K, a $\chi T$ plateau is reached with a maximum value of 5.2 cm$^3$Kmol$^{-1}$, which corresponds to an $S_{\mathrm{T}} = {}^5/_2$ ground state ($g_{S_{\mathrm{T}}=5/2} = 2.18(5)$). In this system, the ferromagnetic coupling is straightforward to rationalize considering the orthogonality of the Ni magnetic orbitals ($d_{x^2-y^2}$ and $d_{z^2}$, Figure S4)[14] and the bridging ligand SOMO which is delocalized on the π system. Using an isotropic spin Heisenberg model,[15] its magnitude was estimated[13] to be $J_{\mathrm{Ni\text{-}rad}}/k_{\mathrm{B}}$=+214(5) K ($g = 2.17(5)$; Figure S9) leading to an energetically well isolated $S_{\mathrm{T}} = {}^5/_2$ ground state (the first $S = {}^3/_2$ excited state lies at 214 K above). This large coupling, that is in good agreement with the calculated one (+249 K; DFT; Supporting Information),[9] is significantly stronger than what was observed in other radical bridged Ni(II) complexes,[16] as likely the consequence of the strong metal-ligand coordination revealed experimentally by the short Ni-N2 bond distance.

For the doubly-reduced compound **3**, the magnetic susceptibility data are similar to **1** with a constant $\chi T$ product at *ca.* 2.3 cm$^3$Kmol$^{-1}$ between 300 and 25 K (Figures 4 & S10), which is expected for a Curie behavior with two Ni(II) spins ($g_{\mathrm{Ni}} = 2.14(5)$). As suggested by X-ray diffraction and spectroscopic measurements, the magnetic properties conclude unambiguously that the Ni oxidation and spin states do not change after successive reductions. Upon cooling below 25 K, the $\chi T$ value decreases to 1.5 cm$^3$Kmol$^{-1}$ at 1.85 K. Like in **1**, this low temperature behavior is probably the result of the combined contributions from the weak intramolecular AF interaction (estimated by DFT at -2.2 K)[9] and the Ni magnetic anisotropy. The $\chi T$ vs $T$ and $M$ vs $H$ fits[12,13] lead systematically to $J_{\mathrm{Ni\text{-}Ni}}$ values close to zero ($|J_{\mathrm{Ni\text{-}Ni}}/k_{\mathrm{B}}| < 0.1$ K) with $g_{\mathrm{Ni}} = 2.14(5)$ and $D_{\mathrm{Ni}}/k_{\mathrm{B}} = -10.4(3)$K (solid lines in Figures 4 & S10). Despite the presence of a significant magnetic anisotropy, no out-of-phase ac signal was detected above 1.85 K and up to 10 kHz for these compounds.

This new series of complexes with different redox states offers the appealing opportunity for a direct comparison between Ni(II) and Co(II) analogues, for which only the metal electronic configuration differs. Indeed, the once and twice reduced forms of the Ni and Co complexes are quasi-isometric, providing a unique platform to directly probe the influence of the singly-occupied atomic orbitals of the metal ion on the strength and sign of the magnetic coupling. According to the ab initio ligand field theory, the Ni(II) unpaired electrons are formally located on the $d_{x^2-y^2}$ and $d_{z^2}$ orbitals (Figure S4),[14] which are only weakly interacting with tphz nitrogen σ-orbitals (Figures S5 & S7). In this situation, the spin density is, as expected, mostly located on the metal ions in **1** and **3** (Figure 4) and the magnetic interactions between the two Ni(II) spins are necessarily weak. Moreover, those metal ion singly-occupied orbitals are orthogonal to the ligand π system. Therefore, as already mentioned, when the tphz$^{\bullet-}$ radical is stabilized in **2**, the unpaired electron is located on the ligand π orbital and a remarkably large ferromagnetic coupling is observed between metal and radical spins.

In the *hs*-Co(II) analogues, in addition to the two unpaired electron located on the $d_{x^2-y^2}$ and $d_{z^2}$ orbitals, a third one is available on the $d_{xy}$ orbital. This different electronic configuration has a considerable impact on the magnetism,[4] as $d_{xy}$ is the only orbital with an orientation that allows a significant overlap with the ligand π system. Hence, this efficient mixing of the $d_{xy}$ and π orbitals induces an efficient spin density delocalization in the *hs*-Co(II) complexes. When twice reduced, tphz$^{2-}$ is formally diamagnetic, but the large spin delocalization promotes a strong AF coupling between the two Co(II) (-74 K), in striking contrast to **3**.[17] This comparative study demonstrates the key role of the $d_{xy}$ orbital on the strength of the intramolecular magnetic exchange.

At least one order of magnitude is also gained on the magnetic interaction, when a single electron is located on the ligand π orbital. The metal ion and tphz$^{\bullet-}$ spins are strongly ferromagnetically coupled in the Ni(II) case with $J/k_{\mathrm{B}} = +214$ K (*vide supra*), while a huge antiferromagnetic exchange is observed for the *hs*-Co(II) complex (at least -500 K). The $J(d_{xy}/\pi)$ coupling between the $d_{xy}$ and π unpaired electrons is thus very large as it overcomes the ferromagnetic $J(d_{x^2-y^2}/\pi)$ and $J(d_{z^2}/\pi)$ contributions. Qualitatively, the $J(d_{xy}/\pi)$ interaction is thus larger than -700 K from the simple $J_{\mathrm{co\text{-}rad}}/k_{\mathrm{B}}$ - $J_{\mathrm{Ni\text{-}rad}}/k_{\mathrm{B}}$ relation.[18]

In conclusion, this work reports on a new series of dinuclear $[(\mathrm{tpy})\mathrm{Ni}(\mathrm{tphz})\mathrm{Ni}(\mathrm{tpy})]^{n+}$ complexes which provides, in comparison to the *hs*-Co(II) analogues, a complete set of experimental and theoretical results allowing a general understanding of the dominant factors governing the strength and nature of the magnetic coupling via an aromatic bridging ligand. In particular, in addition to the obvious interest of using a radical bridging ligand, the careful selection of the metal ion based on its electronic configuration is the key step to promote the strongest possible coupling: this is happening when the unpaired electrons reside on the suitable $t_{2g}$ orbitals, which overlap the best with the radical π system. This general approach should be easily transposed to systems with higher nuclearities and dimensionalities, for which strong magnetic exchanges could be fully exploited to design high temperature molecule-based magnets.[10,19]

## ■ ASSOCIATED CONTENT

### Ⓢ Supporting Information

The Supporting Information is available free of charge on the ACS Publications website at DOI:

Experimental details about syntheses, structural, optical characterizations and theoretical calculations (PDF)
X-ray crystallographic data for **1**-**3** (CIF)

## ■ AUTHOR INFORMATION

### Corresponding Authors

*dechambenoit@crpp-bordeaux.cnrs.fr
*clerac@crpp-bordeaux.cnrs.fr

### ORCID

Elizaveta A. Suturina: 0000-0003-4407-1882
Rodolphe Clérac: 0000-0001-5429-7418
Pierre Dechambenoit: 0000-0001-7850-2260

### Notes

The authors declare no competing financial interests.

## ■ ACKNOWLEDGMENTS

This work was supported by the ANR (ANR-16-CE29-0001-01, Active-Magnet project), the University of Bordeaux, the Région Nouvelle Aquitaine, the CNRS, the MOLSPIN COST action CA15128 and the Chinese Scholarship Council (CSC) for the PhD funding of XM. EAS thanks EPSRC for support (EP/N006895/1), the IRIDIS High Performance Computing Facility and associated services at the University of Southampton and RSC for travel grant. The authors thank also S. De, D. Woodruff, P. Perlepe, I. Oyarzabal and S. Exiga for their assistance and fruitful discussions as well as the GdR MCM-2.

## ■ REFERENCES

(1) (a) Verdaguer, M.; Bleuzen, A.; Marvaud, V.; Vaissermann, J.; Seuleiman, M.; Desplanches, C.; Scuiller, A.; Train, C.; Garde, R.; Gelly, G.; Lomenech, C.; Rosenman, I.; Veillet, P.; Cartier C.; Villain, F. Molecules to build solids: high $T_C$ molecule-based magnets by design and recent revival of cyano complexes chemistry. *Coord. Chem. Rev.* **1999**, *190–192*, 1023-1047. (b) Weihe, H.; Güdel, H. U. Magnetic exchange across the cyanide bridge. *Comments Inorg. Chem.* **2000**, *22*, 75-103. (c) Ruiz E.; Rodriguez-Fortea, A.; Alvarez S.; Verdaguer, M. Is it possible to get high $T_C$ magnets with Prussian blue analogues? A theoretical prospect. *Chem.–Eur. J.* **2005**, *11*, 2135-2144.

(2) (a) Bechlars, B.; D'Alessandro, D. M.; Jenkins, D. M.; Iavarone A. T.; Glover, S. D.; Kubiak, C.P.; Long, J. R. High-spin ground states via electron delocalization in mixed-valence imidazolate-bridged divanadium complexes. *Nat. Chem.* **2010**, *2*, 362-368. (b) Gaudette, A. I.; Jeon, I.-R.; Anderson, J. S.; Grandjean, F.; Long G. J.; Harris, T. D. Electron hopping through double-exchange coupling in a mixed-valence diiminobenzoquinone-Bridged $Fe_2$ Complex. *J. Am. Chem. Soc.* **2015**, *137*, 12617-12626.

(3) (a) Iwamura, H.; Inoue, K.; Hayamizu, T. High-spin polynitroxide radicals as versatile bridging ligands for transition metal complexes with high ferri/ferromagnetic $T_C$. *Pure & Appl. Chem.* **1996**, *68*, 243-252. (b) Rinehart, J. D.; Fang, M.; Evans, W. J.; Long, J. R. A $N_2^{3-}$ radical-bridged terbium complex exhibiting magnetic hysteresis at 14 K. *J. Am. Chem. Soc.* **2011**, *133*, 14236-14239. (c) Fortier, S.; Le Roy, J. J.; Chen, C.-H.; Vieru, V.; Murugesu, M.; Chibobaru, L. F.; Mindiola, D. J.; Caulton, K. G. A dinuclear cobalt complex featuring unprecedented anodic and cathodic redox switches for single-molecule magnet activity. *J. Am. Chem. Soc.* **2013**, *135*, 14670-14678. (d) Jeon, I.-R.; Park, J. G.; Xiao, D. J.; Harris, T. D. An azophenine radical-bridged $Fe_2$ single-molecule magnet with record magnetic exchange coupling. *J. Am. Chem. Soc.* **2013**, *135*, 16845-16848. (e) Demir, S.; Nippe, M.; Gonzalez, M. I.; Long, J. R. Exchange coupling and magnetic blocking in dilanthanide complexes bridged by the multi-electron redox-active ligand 2,3,5,6-tetra(2-pyridyl)pyrazine. *Chem. Sci.* **2014**, *5*, 4701-4711. (f) DeGayner, J. A.; Jeon, I.-R.; Harris, T. D. A series of tetraazalene radical-bridged $M_2$ ($M = Cr^{III}, Mn^{II}, Fe^{II}, Co^{II}$) complexes with strong magnetic exchange coupling. *Chem. Sci.* **2015**, *6*, 6639-6648. (g) Demir, S.; Jeon, I.-R.; Long, J. R.; Harris, T. D. Radical ligand-containing single-molecule magnets. *Coord. Chem. Rev.* **2015**, *289*, 149-176. (h) Moilanen, J. O.; Chilton, N. F.; Day, B. M.; Pugh, T.; Layfield, R. A. Strong exchange coupling in a trimetallic radical-bridged cobalt(II)-hexaazatrinaphthylene complex. *Angew. Chem. Int. Ed.* **2016**, *55*, 5521-5525. (i) Wang, J.; Li, J.-N.; Zhang, S.-L.; Zhao, X.-H.; Shao, D.; Wang, X.-Y. Syntheses and magnetic properties of a pyrimidyl-substituted nitronyl nitroxide radical and its cobalt(II) complexes. *Chem. Commun.* **2016**, *52*, 5033-5036. (j) Dolinar, B. S.; Gómez-Coca, S.; Alexandropoulos, D. I.; Dunbar, K. R. An air stable radical-bridged dysprosium single molecule magnet and its neutral counterpart: redox switching of magnetic relaxation dynamics. *Chem. Commun.* **2017**, *53*, 2283-2286. (k) Gould, C. A.; Darago, L. E.; Gonzalez, M. I.; Demir, S.; Long, J. R. A trinuclear radical-bridged lanthanide single-molecule magnet. *Angew. Chem. Int. Ed.* **2017**, *56*, 10103-10107. (l) Demir, S.; Gonzalez, M. I.; Darago, L. E.; Evans, W. J.; Long, J. R. Giant coercivity and high magnetic blocking temperatures for $N_2^{3-}$ radical-bridged dilanthanide complexes upon ligand dissociation. *Nat. Comm.* **2017**, *8*, 2144. (m) Dolinar, B. S.; Alexandropoulos, D. I.; Vignesh, K. R.; James, T. A.; Dunbar, K. R. Lanthanide triangles supported by radical bridging ligands. *J. Am. Chem. Soc.* **2018**, *140*, 908-911. (n) Lemes, M. A.; Stein, H. N.; Gabidullin, B.; Robeyns, K.; Clérac, R.; Murugesu, M. Probing magnetic-exchange coupling in supramolecular squares based on reducible tetrazine-derived ligands. *Chem. Eur. J.* **2018**, *24*, 4259-4253.

(4) Ma, X.; Suturina, E. A.; De, S.; Négrier, P.; Rouzières, M.; Clérac, R.; Dechambenoit, P. A redox-active bridging ligand to promote spin delocalization, high-spin complexes, and magnetic multi-switchability. *Angew. Chem. Int. Ed.* **2018**, *57*, 7841-7845.

(5) Iwamura, H.; Koga, N. Molecular approaches to photomagnetic materials. Metal-dependent regiospecificity in the exchange coupling of magnetic metal ions with free radical substituents on pyridine base ligands. *Pure & Appl. Chem.* **1999**, *71*, 2, 231-238.

(6) Lions, F.; Dance, I. G.; Lewis, J. Mono-chelate complexes of pyridine-2-aldehyde 2'-pyridylhydrazone. *J. Chem. Soc. A*, **1967**, 565-572.

(7) The one electron process was confirmed by measuring the rest potential of solutions of **1** and **2**, respectively 0 V and -0.7 V, prior recording the cyclic voltammograms which were found to be identical.

(8) (a) Bonhôte, P.; Lecas, A.; Amouyal, E. Bi-and tri-nuclear ruthenium(II) complexes containing tetrapyridophenazine as a rigid bridging ligand. *Chem. Commun.* **1998**, *8*, 885-886. (b) Gourdon, A.; Launay, J.-P. Mononuclear and binuclear tetrapyrido[2,3-a:3‘,2‘-c:2“,3“-h:3‘“,2‘“-j]phenazine (tphz) ruthenium complexes. *Inorg. Chem.* **1998**, *37*, 5336-5341.

(9) Neese, F. The ORCA program system. *WIREs Comput. Mol. Sci.* **2012**, *2*, 73-78.

(10) Pedersen, K. S.; Perlepe, P.; Aubrey, M. L.; Woodruff, D. N.; Reyes-Lillo, S. E.; Reinholdt, A.; Voigt, L.; Li, Z.; Borup, K.; Rouzières, M.; Samohvalov, D.; Wilhelm, F.; Rogalev, A.; Neaton, J. B., Long, J. R.; Clérac, R. Formation of the layered conductive magnet $CrCl_2(pyrazine)_2$ through redox-active coordination chemistry. *Nat. Chem.* **2018**, *10*, 1056-1061.

(11) (a) Pickering, I. J.; George, G. N.; Lewandowski, J. T.; Jacobson, A. J. Nickel K-edge X-ray absorption fine structure of lithium nickel oxides. *J. Am. Chem. Soc.* **1993**, *115*, 4137-4144. (b) Szilagyi, R. K.; Lim, B. S.; Glaser, T.; Holm, R. H.; Hedman, B.; Hodgson, K. O.; Solomon, E. I. Description of the ground state wave functions of Ni dithiolenes using sulfur K-edge X-ray absorption spectroscopy. *J. Am. Chem. Soc.* **2003**, *125*, 9158-9169. (c) Perlepe, P.; Oyarzabal, I.; Pedersen, K.S.; Negrier, P.; Mondieig, D.; Rouzières, M.; Hillard, E.A.; Wilhelm, F.; Rogalev, A.; Suturina, E.A.; Mathonière C.; Clérac, R. $Cr(pyrazine)_2(OSO_2CH_3)_2$: a two-dimensional coordination polymer with an antiferromagnetic ground state. *Polyhedron* **2018**, *153*, 248-253. (d) Liang, H. W.; Kroll, T.; Nordlund, D.; Weng, T.-C.; Sokaras, D.; Pierpont, C. G.; Gaffney K.J. Charge and spin-state characterization of cobalt bis(o-dioxolene) valence tautomers using Co $K\beta$ X-ray emission and L-Edge X-ray absorption spectroscopies. *Inorg. Chem.* **2017**, *56*, 737-747. (e) Koroidov, S.; Hong, K.; Kjaer, K. S.; Li, L.; Kunnus, K.; Reinhard, M.; Hartsock, R. W.; Amit, D.; Eisenberg, R.; Pemmaraju, C.D.; Gaffney, K.; Cordones, A. A. Probing the electron accepting orbitals of Ni-centered hydrogen evolution catalysts with noninnocent ligands by Ni L-edge and S K-edge X-ray absorption. *Inorg. Chem.* **2018**, *57*, 13167-13175. (f) Jafri, S. F.; Koumousi, E. S.; Arrio, M.-A.; Juhin, A.; Mitcov, D.; Rouzières, M.; Dechambenoit, P.; Li, D.; Otero, E.; Wilhelm, F.; Rogalev, A.; Joly, L.; Kappler, J.-P.; Moulin, C. C. D.; Mathonière, C.; Clérac, R.; Sainctavit, P. Atomic scale evidence of the switching mechanism in a photomagnetic CoFe dinuclear Prussian blue analogue. *J. Am. Chem. Soc.* **2019**, *141*, 3470-3479.

(12) The following Hamiltonian has been used to fit the magnetic data:
$$\hat{H} = -2J_{Ni-Ni}(\vec{S}_{Ni1} \cdot \vec{S}_{Ni2}) + 2D_{Ni}S_{Ni,z}^2 + 2g_{Ni}\mu_B\vec{S}_{Ni} \cdot \vec{H}$$

(13) Chilton, N. F.; Anderson, R. P.; Turner, L. D.; Soncini, A.; Murray, K. S. PHI: a powerful new program for the analysis of anisotropic monomeric and

exchange-coupled polynuclear d- and f-block complexes. *J. Comput. Chem.* **2013**, *34*, 1164-1175.

(14) The average N1-Ni-N3 axis is taken as the $z$ direction by convention (Figure 1).

(15) The following Hamiltonian has been used to fit the magnetic data:

$$\hat{H} = -2J_{Ni-rad}(\vec{S}_{Ni1} + \vec{S}_{Ni2}) \cdot \vec{S}_{rad} + \mu_B(2g_{Ni}\vec{S}_{Ni} + g_{rad}\vec{S}_{rad}) \cdot \vec{H}$$

(16) (a) Dei, A.; Gatteschi, D.; Pardi, L. Sextet ground state in a dinuclear nickel(II) complex containing a tetraoxolene radical as bridging ligand. *Inorg. Chim. Acta* **1991**, *189*, 125-128. (b) Woods, T. J.; Stout, H. D.; Dolinar, B. S.; Vignesh, K. R.; Ballesteros-Rivas, M. F.; Achim, C.; Dunbar, K. R. Strong ferromagnetic exchange coupling mediated by a bridging tetrazine radical in a dinuclear nickel complex. *Inorg. Chem.* **2017**, *56*, 12094-12097. (c) Lemes, M. A.; Brunet, G.; Pialat, A.; Ungur, L.; Korobkova, I.; Korobkov, I.; Murugesu, M. Strong ferromagnetic exchange coupling in a $\{Ni^{II}_4\}$ cluster mediated through an air-stable tetrazine-based radical anion. *Chem. Commun.* **2017**, *53*, 8660-8663.

(17) This is further confirmed by UV-vis-NIR spectrometry which reveals the absence of an absorption band in the NIR region for **3** (Figure S3) in contrast to its Co analogue (reference 4).

(18) More accurately, this $J(d_{xy}/\ \pi)$ antiferromagnetic coupling is better described as being between the $d_{xy}$(Co)+π($N_{tphz}$) orbital and the $\pi$ system of the carbon atoms of the tphz pyrazine part (for symmetry reasons of the involved orbitals).

(19) (a) Manriquez, J. M.; Yee, G. T.; McLean, R. S.; Epstein, A. J.; Miller, J. S. A room-temperature molecular/organic-based magnet. *Science* **1991**, *252*, 1415-1417. (b) Miller J. S. Magnetically ordered molecule-based materials. *Chem. Soc. Rev.* **2011**, *40*, 3266-3296. (c) Miller J. S., Ohkoshi, S.-i. in *High-$T_C$ Ordered Molecular Magnets in* Molecular Magnetic Materials: Concepts and Applications; Eds. Sieklucka, B.; Pinkowicz, D., Wiley–VCH: Wienheim, 2017.

## Table of Content Artwork